



# Journal of the European Ceramic Society

journal homepage: [www.elsevier.com/locate/jeurceramsoc](http://www.elsevier.com/locate/jeurceramsoc)



## Sintering behavior and characteristics study of BaTiO<sub>3</sub> with 50 wt% of B<sub>2</sub>O<sub>3</sub>-Bi<sub>2</sub>O<sub>3</sub>-SiO<sub>2</sub>-ZnO glass

Mei-Yu Chen <sup>a,\*</sup>, Jari Juuti <sup>a</sup>, Chi-Shiung Hsi <sup>b</sup>, Heli Jantunen <sup>a</sup>

<sup>a</sup> Microelectronics Research Unit, Faculty of Information Technology and Electrical Engineering, P.O. Box 4500, FI-90014, University of Oulu, Finland

<sup>b</sup> Department of Material Science and Engineering, National United University, Miao-Li, 36003, Taiwan

### ARTICLE INFO

#### Article history:

Received 15 July 2016

Received in revised form 26 October 2016

Accepted 31 October 2016

Available online xxx

#### Keywords:

Glass-ceramic composite

BBSZ

BaTiO<sub>3</sub>

Sintering behavior

Dielectric properties

### ABSTRACT

The thermal analysis of B<sub>2</sub>O<sub>3</sub>-Bi<sub>2</sub>O<sub>3</sub>-SiO<sub>2</sub>-ZnO (BBSZ) glass with different particle sizes and LiF addition was researched to study its temperature behavior. Next the composites with 50 wt% BaTiO<sub>3</sub>-50 wt% BBSZ glass were prepared for shrinkage, microstructures and dielectric properties investigations. The differently treated BBSZ glass showed that the smaller glass particles clearly decreased its softening and crystallization temperatures. LiF addition had the same but much weaker effect.

The composites showed two-stage shrinkage related to the softening of the glass and new phase generation of Bi<sub>24</sub>Si<sub>2</sub>O<sub>40</sub> at 385–450 °C, and Bi<sub>4</sub>BaTi<sub>4</sub>O<sub>15</sub> over 680 °C. The microstructures of the composites sintered at 720 °C showed Bi<sub>4</sub>BaTi<sub>4</sub>O<sub>15</sub>, BaTiO<sub>3</sub> and Bi<sub>24</sub>Si<sub>2</sub>O<sub>40</sub> with residual ZnO phase. LiF addition increased the amount of Bi<sub>4</sub>BaTi<sub>4</sub>O<sub>15</sub>, thus increasing the loss value. However the particle size of the glass did not effect to the dielectric properties of the composites showing permittivity of 248–256 and loss of 0.013 at 100 kHz.

© 2016 Published by Elsevier Ltd.

## 1. Introduction

Glass-ceramic composite (glass + ceramic) and glass-ceramics (crystallizing glass) are two important approaches to develop Low Temperature Cofired Ceramics (LTCCs). These materials having application optimized dielectric properties, high mechanical strength, high chemical durability, and low thermal expansion, are applied in many multilayer microwave components and packages. Crystallizing cordierite by IBM and wollastonite by Ferro are the examples for glass-ceramic systems [1]. Recently, ULTCCs (Ultra-Low Temperature Cofired Ceramics) have attracted the scientists' attention since the targeted sintering temperatures are low (<700 °C) thus enabling low energy consumption and integration with plastic or semiconductors to create diverse applications [2–4]. Also in LTCC technology the glass/ceramic composites with low transition temperature ( $T_g$ ) glass is a feasible approach. B<sub>2</sub>O<sub>3</sub>-Bi<sub>2</sub>O<sub>3</sub>-SiO<sub>2</sub>-ZnO (BBSZ) glass, used in many LTCCs, has a low transition temperature [5,6]. In LTCC technology also several other methods to decrease the sintering temperature has been used, such as enlarging surface area of particles, glass coating, and addition of fluoride [7,8]. Hsi et al. reported that calcium borosilicate glass coated BaTiO<sub>3</sub> enabled efficient decrease of sintering temperature from 1450 °C to 850 °C [7]. In addition, a small amount of LiF was

added to decrease the transition temperature of the glass [8]. Wang et al. [9] revealed that below sintering temperature of 920 °C the linear shrinkage rate of BaO-B<sub>2</sub>O<sub>3</sub>-SiO<sub>2</sub>/BaTiO<sub>3</sub> glass ceramics reached about 10% when the amount of BaTiO<sub>3</sub> in range of 60–90 wt%. The permittivity are adjustable from 5 to 30 at 100 MHz with 60–90 wt% amount of BaTiO<sub>3</sub>. The glass ceramics with high glass content, such as composition of BaTiO<sub>3</sub> with 70–90 wt% BBSZ glass [10], can be sintered at ultra-low sintering temperature (450 °C), and exhibit high permittivity of 132 and low loss of 0.006 at 100 kHz.

In this paper the main goal is to research how high permittivity values are achievable if the amount of BBSZ glass in the BBSZ-BaTiO<sub>3</sub> composite is decreased to 50 wt%. Thermal analysis of the bulk and powder samples of BBSZ with different particle sizes and LiF addition are also performed for deeper understanding of its behavior at different temperatures. This is important not only for this study related to BBSZ-BaTiO<sub>3</sub> composites, but also for future utilization of the glass.

## 2. Experiment

The BBSZ glass was prepared by using analysis grade chemicals of 27 mol % of B<sub>2</sub>O<sub>3</sub>, 35 mol % of Bi<sub>2</sub>O<sub>3</sub>, 6 mol % of SiO<sub>2</sub> and 32 mol % of ZnO. The mixed raw materials were melted in a platinum crucible at 900 °C for one hour. The melt was quenched in water to form an amorphous glass, dried and crushed. Planetary milling for 24 h with zirconia balls was applied with deionized water. The mean particle size of the glass powder was 1 μm. Another batch of the glass pow-

\* Corresponding author.

E-mail addresses: [mchen@ee.oulu.fi](mailto:mchen@ee.oulu.fi), [chenmyphy@gmail.com](mailto:chenmyphy@gmail.com) (M.-Y. Chen).

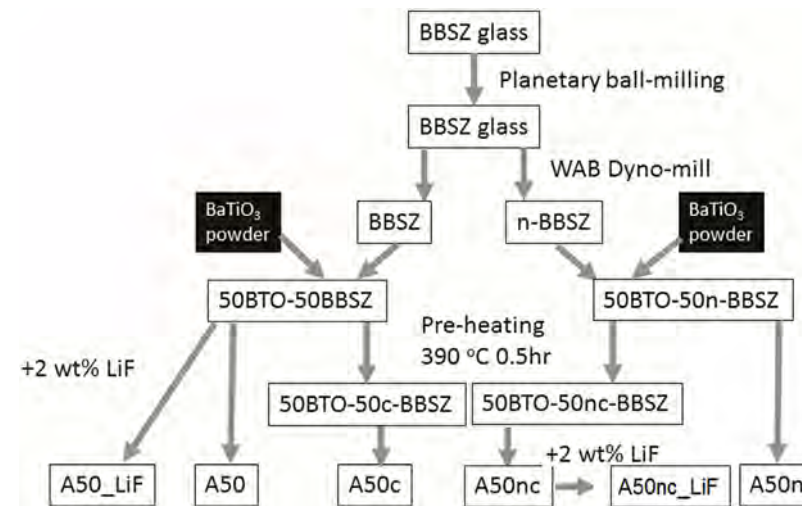


Fig. 1. Samples preparation routes.

der (n-BBSZ) to achieve smaller particle size ( $D_{50} = 0.52 \mu\text{m}$ ) was prepared by a Dyno-mill(WAB DYNOMILL, Switzerland) with 0.3 mm zirconia balls. Differential scanning calorimetric (Netzsch 404 F3, Germany) measurements for BBSZ glass with different particle sizes were performed.  $\text{BaTiO}_3$  powder (purity > 99.7%, Alfa Aesar) was used as a dielectric properties modifier by mixing for 4 h it to BBSZ and n-BBSZ glasses in ethanol solution with small amount of fish oil as a dispersant. After drying, these two batches were divided into three powder samples. The first sample was pressed into  $\varnothing = 10 \text{ mm}$  pellet and directly sintered, while the second one was pre-heated at 390 °C for 0.5 h and then pressed into pellets and sintered. The third powder sample was mixed with 2 wt% LiF, pressed into pellets and sintered. The same procedure was performed in both cases of the BBSZ glass. The green densities of all specimens were 50–60% of their theoretical densities. The samples were sintered at 450 °C for a half an hour and at 720 °C for 5 h with a heating rate of 3 °C/min using conventional sintering process. The preparation routes of the samples are depicted in Fig. 1. The sintered densities were measured by Archimedes method. The sintering temperature of the samples was studied using dilatometer (Netzsch DIL402-PC, Germany), and the microstructures and the phases of the sintered samples were studied by FESEM (ZEISS Ultra Plus, Germany) and X-ray diffraction measurements (XRD, Bruker D8, Cu,  $K\alpha \sim 1.54 \text{ \AA}$ , MA, USA and XRD, Rigaku, Co,  $K\alpha \sim 1.79 \text{ \AA}$ , Tokyo, Japan). The dielectric properties at 100 kHz were measured by Precision LCR meter (LCR, HP 4284, USA) using sputtered silver electrodes.

### 3. Results and discussion

The behavior of the BBSZ glass powder and bulk samples as a function of temperature was studied with the scanning calorimetric and the differential curves (Fig. 2). Very weak peaks at around 382–386 °C indicate that the transition temperatures ( $T_g$ ) of the BBSZ glass with mean particle size of 1  $\mu\text{m}$  and 0.5  $\mu\text{m}$  (denoted as n-BBSZ) are about the same. The softening temperature ( $T_s$ ) for these BBSZ and n-BBSZ glasses is 416 °C, while the addition of LiF decreases it to 408 °C. The exothermal peaks representing the crystallization temperature of the glass are 483 °C for the BBSZ bulk, and 462 and 430 °C for the BBSZ and n-BBSZ powders, respectively. This shows that the particle size has a strong influence on crystallization. Furthermore, the addition of LiF further decreases the  $T_c$  of n-BBSZ to the value of 423 °C.

The dilatometer curves in Fig. 3 reveal the shrinkage behaviors of all 50 wt%  $\text{BaTiO}_3$ –50 wt% BBSZ composite, A50 denoting sample with common size glass particles, A50n sample with small glass particles, A50-LiF common size glass particles with LiF addition, A50c common size particles preheated at 390 °C, A50nc sample with small glass particles preheated at 390 °C, and A50nc\_LiF being the latest one but with LiF addition.

As previously reported [9], the sintering of A50 sample at 450 °C exhibited low density and high porosity. Through the dilatometer measurements, not only suitable sintering temperature can be obtained, but also interactions between the glass and  $\text{BaTiO}_3$  can be studied separately. In Fig. 3(b), the derivations of the dilatometer curves show that two main shrinkage phases occur at around 400 °C and 700 °C. The shrinkage around 400 °C is attributed to the softening and rearrangement of the glass particle, which are in correlation with the DSC results. When the temperature increases at 720 °C, almost fully densification of samples is achieved. Furthermore, the shrinkage behavior of different  $\text{BaTiO}_3$ -BBSZ composites is somewhat different. A50 sample presents typical conventional process with two peaks at 400 and 422 °C, and a stronger one at 718 °C. Different composite treatments change the onset and maximum value of shrinkage rate as shown in Table 1. The A50 and A50c samples show similar peak shapes. Both of them have high intensity peak at 427 °C referring to high portion of the secondary phase  $\text{Bi}_{24}\text{Si}_2\text{O}_{40}$  also confirmed by XRD later on. The lower onset temperature of the A50c sample indicates that with the pre-heating the sintering starts a little earlier due to the lower surface tension, but it does not decrease the sintering temperature or change the sintering mechanism. The small size glass particles are expected to surround the  $\text{BaTiO}_3$  particles more uniformly, to decrease the distance between  $\text{BaTiO}_3$  particles, and enhance the capillary pressure. However, the composite with small glass particles show only slight decrease in the sintering temperature.

The A50, A50c, A50\_LiF, and A50n, A50nc, A50nc\_LiF samples sintered at 720 °C for 5 h have high density (~6.0 g/cm<sup>3</sup>) with low porosity (<2%), unlike in the case when the sintering was performed at 450 °C. The XRD patterns of the pure BBSZ glass and BBSZ- $\text{BaTiO}_3$  composites sintered at 450 °C and 720 °C are shown in Fig. 4. The Co target was used for the composites sintered at 720 °C in order to obtain higher accuracy. For pure BBSZ glass, the weak peaks assigned as  $\text{Bi}_{24}\text{Si}_2\text{O}_{40}$  phase are observed after sintering at 450 °C, and  $\text{Zn}_2\text{SiO}_4$  phase in amorphous hump at 20–35° after sintering at 720 °C. The  $\text{BaTiO}_3$  (peaks denoted with stars) can be clearly observed in A50 sample sintered at 450 °C.

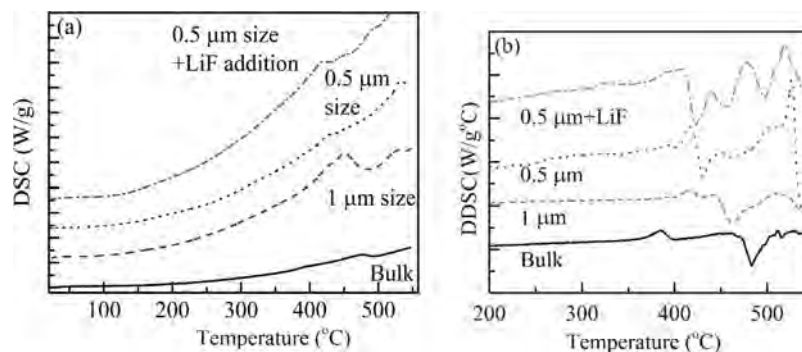


**Fig. 2.** (a) DSC and (b) differential curves of BBSZ glass with different particle size and LiF addition.

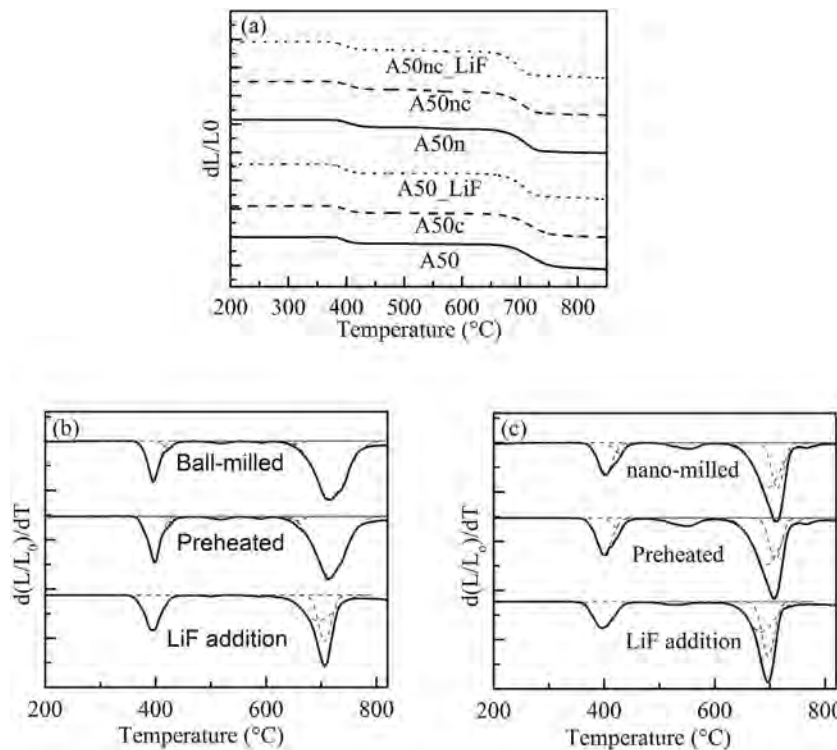


**Fig. 3.** (a) Dilatometric curves of 50BaTiO<sub>3</sub>–50 wt% BBSZ glass composite with different procedure, (b) and their derivation which were analyzed by Gaussian peaks.

**Table 1**

Analyses of dilatometric curves (onset point) and their differential values (peaks).

samples	onset point	peak position	peak position	onset	peak position	peak position
A50	388	396	422	687	NA	718
A50c	383	397	426	682	NA	716
A50_LiF	377	395	NA	685	694	706
A50n	385	402	427	679	695	714
A50nc	382	400	425	675	693	710
A50nc_LiF	376	399	NA	673	684	697

The same peaks of Bi<sub>24</sub>Si<sub>2</sub>O<sub>40</sub> phase, as observed earlier when the amount of BBSZ glass was 70 wt% [9], also appeared for the A50n sample sintered at 450 °C. Furthermore, when the sintering temperature is increased to 720 °C, BBSZ glass melts and zinc silicate (Zn<sub>2</sub>SiO<sub>4</sub>) phase appears. For the BaTiO<sub>3</sub>-BBSZ composites sintered at 720 °C, BaBi<sub>4</sub>Ti<sub>4</sub>O<sub>15</sub>, Ba<sub>24</sub>Si<sub>2</sub>O<sub>40</sub> and zincate ZnO phase are shown in all of samples. Also, a very few amount of barium zinc silicate BaZn(SiO<sub>4</sub>) is observed in the samples with smaller glass size and LiF addition. This result correlated with the two peak around 720 °C in Table 1. Furthermore, the intensities of the Bi<sub>24</sub>Si<sub>2</sub>O<sub>40</sub> and

BaBi<sub>4</sub>Ti<sub>4</sub>O<sub>15</sub> phases greatly increase due to the LiF addition meaning at 720 °C the LiF addition not only enhance the generation of the secondary phases, but also decreases the sintering temperatures in some extent (Table 1). Induja et al. reported that the same BBSZ glass composition with 40 wt% Al<sub>2</sub>O<sub>3</sub> sintered at 850 °C shows the Ba<sub>24</sub>Si<sub>2</sub>O<sub>40</sub> and ZnAl<sub>2</sub>O<sub>4</sub> phase [11]. The similar silicate second phase of Ba<sub>2</sub>TiSi<sub>2</sub>O<sub>8</sub> are also found in BaO-B<sub>2</sub>O<sub>3</sub>-SiO<sub>2</sub>/BaTiO<sub>3</sub> [9] and ZnO-B<sub>2</sub>O<sub>3</sub>-SiO<sub>2</sub>/BaTiO<sub>3</sub> glass ceramic system [12]. Therefore, the interaction between glass and filler is hard to avoid at high heating temperature (>700 °C).

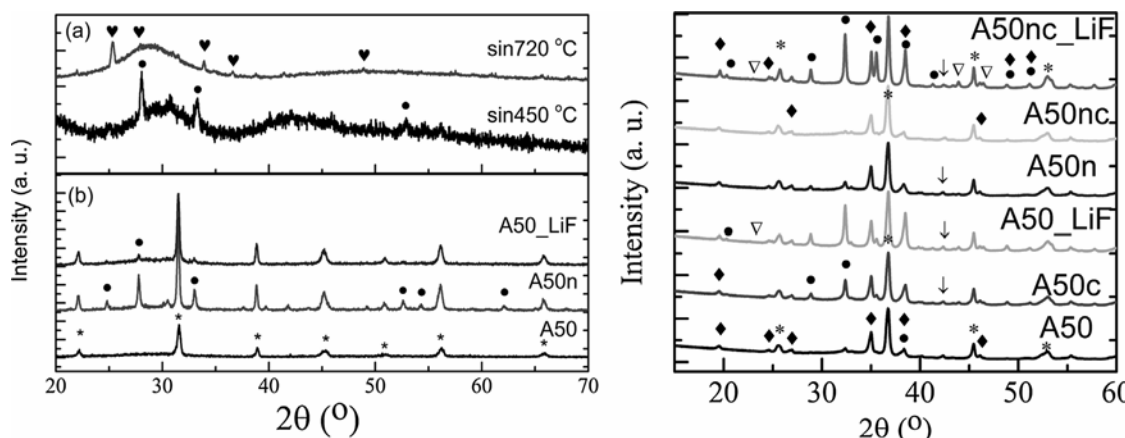


**Fig. 4.** (a) XRD patterns of BBSZ glass sintered at 450 and 720 °C, and (b) composite samples sintered at 450 °C, and (c) at 720 °C (Co target). (\* refer to BaTiO<sub>3</sub>, ● Bi<sub>24</sub>Si<sub>2</sub>O<sub>40</sub>, ▲ Zn<sub>2</sub>SiO<sub>4</sub>, ♦ BaBi<sub>4</sub>Ti<sub>4</sub>O<sub>15</sub>, ↓ ZnO, and ▽ BaZn(SiO<sub>4</sub>).

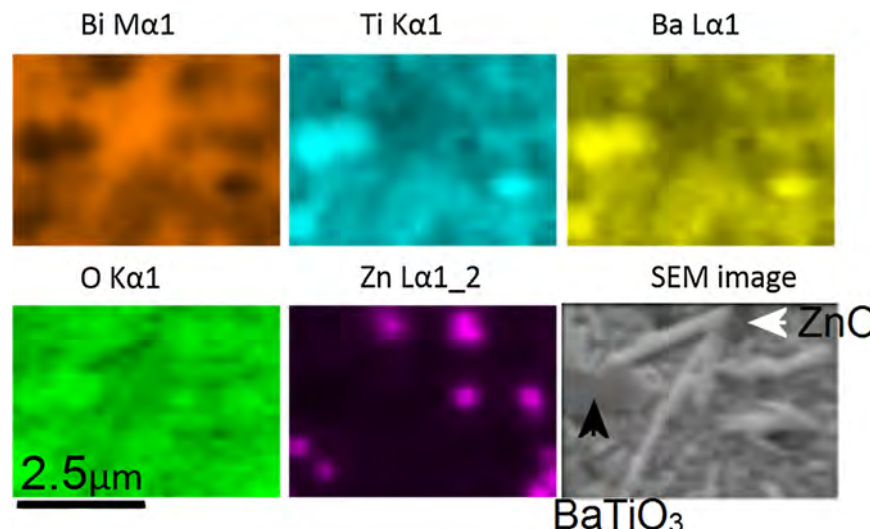


**Fig. 5.** Element mapping of A50 samples sintered at 720 °C.

**Fig. 5** illustrates the element mapping of A50 sample sintered at 720 °C. Through EDS analysis, some BaTiO<sub>3</sub> particles can be identified (left center in the SEM figure) due to the existence of barium, titanium and oxygen, and absence of bismuth element. The area with Zn element in Zn L<sub>α</sub>1\_2 scan can be expected to represent ZnO due to the XRD and EDS results. The backscattering electron images of different samples in **Fig. 6** also clearly show different phases and microstructures of samples with ZnO (black areas), BaTiO<sub>3</sub> phase (dark grey), Bi<sub>4</sub>BaTi<sub>4</sub>O<sub>15</sub> phase (light grey rod-shape), and Bi<sub>24</sub>Si<sub>2</sub>O<sub>40</sub> phase (bright white). The **Fig. 5(c)** and (f) also show that the LiF addition clearly increases the amount of Bi<sub>4</sub>BaTi<sub>4</sub>O<sub>15</sub> and Bi<sub>24</sub>Si<sub>2</sub>O<sub>40</sub>. This is well in line with the earlier results. The ZnO phase tend to form large clusters especially clear in the microstructure of A50nc\_LiF sample. The only exception from this is A50nc samples, where the small size of different phases homogeneously distribute in the dense structures. This indicate the small particle size with pre-heating process for coating at 390 °C inhibit the clustering of particles with different phases.

**Table 2** shows the dielectric properties at 100 kHz for six samples sintered at 720 °C for 5 h. A50 with different glass particle size and coating process have relatively high permittivity of 248–259 with the same tan δ of 0.013. However, small LiF addition on A50 decreased the permittivity to 186–211 and increased the loss value to 0.017–0.018. This dielectric properties can be explained accord-

**Table 2**

Dielectric properties of A50, A50c, A50\_LiF, A50n, A50nc, and A50nc\_LiF sintered 720 °C.

Sintered 720 °C @100 kHz	$\varepsilon_r$	$\tan \delta$
A50	255	0.013 ± 0.001
A50c	248	0.013 ± 0.001
A50_LiF	202	0.017 ± 0.001
A50n	259	0.013 ± 0.001
A50nc	248	0.013 ± 0.001
A50nc_LiF	186	0.018 ± 0.001

ing to the microstructure characteristics and XRD results. They confirm that the amount of BaBi<sub>4</sub>Ti<sub>4</sub>O<sub>15</sub> and Ba<sub>24</sub>Si<sub>2</sub>O<sub>40</sub> is increased and in some extent dominate the microstructure. The Ba<sub>24</sub>Si<sub>2</sub>O<sub>40</sub> single crystal show a low  $\varepsilon_r$  value of 46 and tan δ of 0.005 at 1 MHz [13], and the bulk BaTiO<sub>3</sub> sintered at 1350 °C for 2 h has a high  $\varepsilon_r$  of 1781 and tan δ of 0.003 at 100 kHz. However, the dielectric properties of the BaBi<sub>4</sub>Ti<sub>4</sub>O<sub>15</sub> are difficult to determine due to its highly anisotropic structure and the permittivity of ab- and c-axis has been reported to be 1000 and 110 at 1 kHz, respectively [15]. Also other permittivity values are reported [14–17]. One can however assume that the BaBi<sub>4</sub>Ti<sub>4</sub>O<sub>15</sub> phase is responsible for the high loss values especially in the case of LiF-doped samples. This is because the tan δ for BaTiO<sub>3</sub> is ~0.003 at 100 kHz [10], and for Ba<sub>24</sub>Si<sub>2</sub>O<sub>40</sub> ~0.005 at

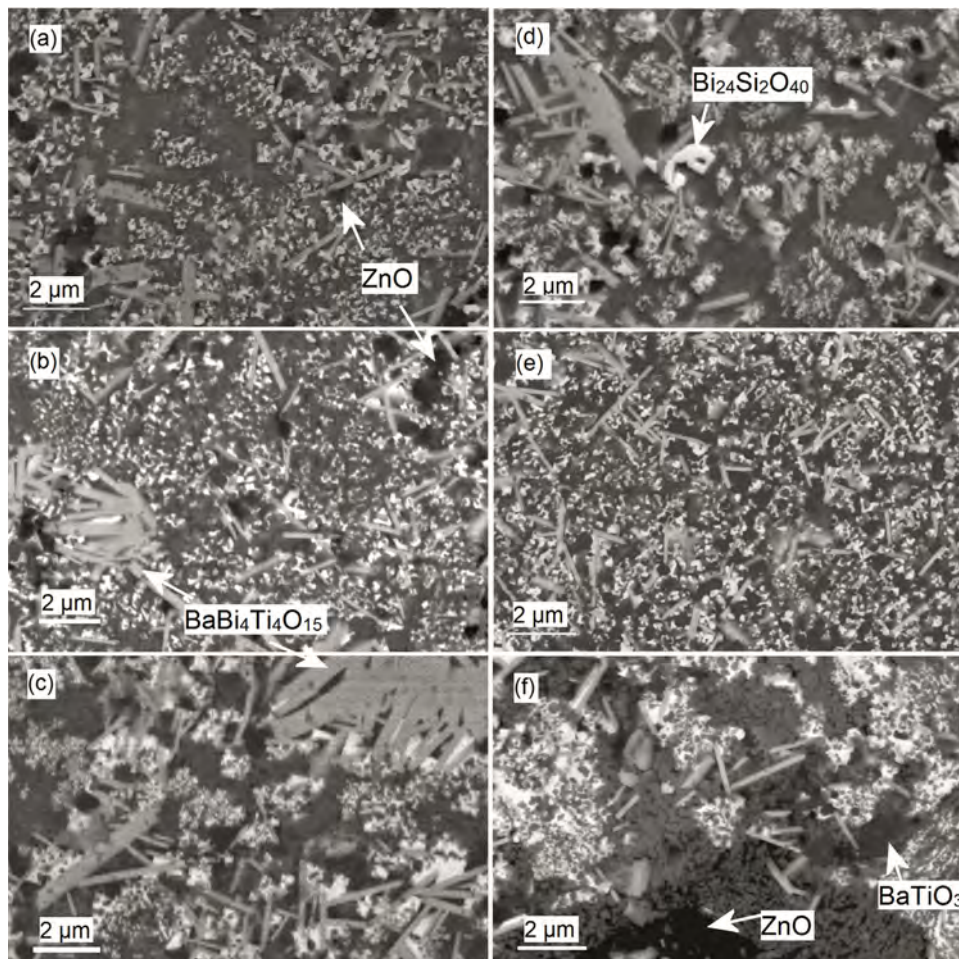


**Fig. 6.** (a) Backscattered electron images A50 and (b) of A50c, (c) A50\_LiF (d) A50n, (e) A50nc, and (f) A50nc\_LiF samples sintered at 720 °C for 5 h. Black areas represent ZnO, dark gray BaTiO<sub>3</sub>, light gray BaBi<sub>4</sub>Ti<sub>4</sub>O<sub>15</sub> and the bright ones Bi<sub>24</sub>Si<sub>2</sub>O<sub>40</sub>.

1 MHz [13], but the reported values for the BaBi<sub>4</sub>Ti<sub>4</sub>O<sub>15</sub> are much high. The tan δ for the BaBi<sub>4</sub>Ti<sub>4</sub>O<sub>15</sub> measured by Cui et al. [16] is ~0.0135 at 1 kHz and by Diao et al., [17] ~0.025 at 1 MHz. It has been also reported that in this kind of Aurivillius perovskite composites the high losses are emerged from its ferroelectric properties [14–17].

#### 4. Conclusion

The sintering behavior, microstructures and dielectric properties of 50 wt% BaTiO<sub>3</sub>- 50 wt% BBSZ composite were studied. The effects of the glass particle size, pre-heating and LiF addition on densification of the composites were revealed. The shrinkage according to the dilatometer measurements show that it happens in two stages, at around 400 °C, and 700 °C. The first shrinkage around 400 °C was referred to the softening of the glass and the generation of the Bi<sub>24</sub>Si<sub>2</sub>O<sub>40</sub>. The second shrinkage was associated with the second phase generation of ZnO, BaZnSiO<sub>4</sub> and Ba<sub>4</sub>BaTi<sub>4</sub>O<sub>15</sub>. Dense but different microstructures and existence of Ba<sub>4</sub>BaTi<sub>4</sub>O<sub>15</sub>, BaTiO<sub>3</sub>, Bi<sub>24</sub>Si<sub>2</sub>O<sub>40</sub>, ZnO phases in backscattering electron images were observed. The same dielectric properties ( $\epsilon_r = 248\text{--}259$ , tan δ = 0.013 at 100 kHz) after sintering at 720 °C were measured to the BaTiO<sub>3</sub>-BBSZ composites regardless of the size of the glass particles. Rather high loss values are assumed to be due to the Ba<sub>4</sub>BaTi<sub>4</sub>O<sub>15</sub> phase. This was even more obvious in the case when LiF was added, since it increases the amount of Ba<sub>4</sub>BaTi<sub>4</sub>O<sub>15</sub>. However, the achieved microstructures were very dense and dielectric prop-

erties feasible for some miniaturization and packaging applications like embedded capacitors where high permittivity is needed. Also co-firing with materials having similar sintering temperature but much lower permittivity would be beneficial, such as Li<sub>3</sub>Al<sub>2</sub>B<sub>2</sub>O<sub>6</sub> [18], BaNd<sub>2</sub>Ti<sub>5</sub>O<sub>14</sub> + La<sub>2</sub>O<sub>3</sub>-B<sub>2</sub>O<sub>3</sub>-TiO<sub>2</sub> [19], and TiTe<sub>3</sub>O<sub>8</sub> ceramic in TiO<sub>2</sub>-TeO<sub>2</sub> system [20].

#### Acknowledgements

The work is supported by the European Research Council (ERC) under the European Union's Seventh Framework Programme (FP7/2007-2013)/ERC Grant agreement (No. 291132). Author JJ acknowledges the funding of the Academy of Finland (project numbers 267573 and 273663). In addition the authors are grateful to the Center of Microscopy and Nanotechnology (CMNT) at the University of Oulu.

#### References

- [1] E.D. Zanotto, A bright future for glass-ceramics, *Am. Ceram. Soc. Bull.* 89 (8) (2010) 19–27.
- [2] Z.M. Dang, J.K. Yuan, J.W. Zha, T. Zhou, S.T. Li, G.H. Hu, Fundamentals, processes and applications of high-permittivity polymer-matrix composites, *Prog. Mater. Sci.* 57 (4) (2012) 660–723.
- [3] W. Jilek, W.K.C. Yung, Embedded components in printed circuit boards: a processing technology review, *Int. J. Adv. Manuf. Technol.* 25 (3–4) (2005) 350–360.
- [4] S. George, M.T. Sebastian, Three-phase polymer-ceramic-metal composite for embedded capacitor applications, *Compos. Sci. Technol.* 69 (7–8) (2009) 1298–1302.

- [5] S. Thomas, M.T. Sebastian, Effect of  $B_2O_3$ - $Bi_2O_3$ - $SiO_2$ - $ZnO$  glass on the sintering and microwave dielectric properties of 0.83ZnAl<sub>2</sub>O<sub>4</sub>-0.17TiO<sub>2</sub>, *Mater. Res. Bull.* 43 (4) (2008) 843-851.
- [6] H. Hsiang, T. Chen, Electrical properties of low-temperature-fired ferrite-dielectric composites, *Ceram. Int.* 35 (2009) 2035-2039.
- [7] C.S. Hsi, Y.C. Chen, H. Jantunen, M.J. Wu, T.C. Lin, Barium titanate based dielectric sintered with a two-stage process, *J. Eur. Ceram. Soc.* 28 (2008) 2581.
- [8] C.S. Hsi, M.Y. Chen, H. Jantunen, F.C. Hsi, T.C. Lin, Sintering of titanate based dielectrics doped with lithium fluoride and calcium borosilicate glass, *Mater. Sci. Poland* 29 (1) (2011) 29.
- [9] K.T. Wang, Y. He, Z.Y. Liang, X.M. Cui, Preparation of LTCC materials with adjustable permittivity based on BaO-B<sub>2</sub>O<sub>3</sub>-SiO<sub>2</sub>/BaTiO<sub>3</sub> system, *Mater. Res. Bull.* 65 (2015) 249-252.
- [10] M.Y. Chen, J. Juuti, C.S. Hsi, C.T. Chia, H. Jantunen, Dielectric BaTiO<sub>3</sub>-BBSZ glass ceramic composition with ultra-low sintering temperature, *J. Eur. Ceram. Soc.* 35 (2015) 139-144.
- [11] I.J. Induja, P. Abhilash, S. Arun, K.P. Surendran, M.T. Sebastian, LTCC tapes based on Al<sub>2</sub>O<sub>3</sub>-BBSZ glass with improved thermal conductivity, *Ceram. Int.* 41 (10) (2015) 13572-13581.
- [12] H.I. Hsiang, C.S. Hsi, C.C. Huang, S.L. Fu, Sintering behavior and dielectric properties of BaTiO<sub>3</sub> ceramics with glass addition for internal capacitor of LTCC, *J. Alloys Compd.* 459 (2008) 307-310.
- [13] Y.R. Reddy, L. Sirdeshmukh, Dielectric behaviour of Bi<sub>12</sub>SiO<sub>20</sub>, *Phys. Status Solidi A* 103 (1987) K157.
- [14] T. Jardiel, A.C. Caballero, M. Villegas, Aurivillus ceramics: Bi<sub>4</sub>Ti<sub>3</sub>O<sub>12</sub>-based piezoelectrics, *J. Ceram. Soc. Jpn.* 116 (4) (2008) 511-518.
- [15] J.D. Bobic, M.M.V. Petrovic, B.D. Stojanovic, Aurivillus BaBi<sub>4</sub>Ti<sub>4</sub>O<sub>15</sub> based compound: structure, synthesis and properties, *Process. Appl. Ceram.* 7 (3) (2013) 97-110.
- [16] Y. Cui, X. Fu, K. Yan, Effects of Mn-doping on the properties of BaBi<sub>4</sub>Ti<sub>4</sub>O<sub>15</sub> bismuth layer structured ceramics, *J. Inorg. Organomet. Polym.* 22 (2012) 82-85.
- [17] C.L. Diao, J.B. Xu, H.W. Zheng, L. Fang, Y.Z. Gu, W.F. Zhang, Dielectric and piezoelectric properties of cerium modified BaBi<sub>4</sub>Ti<sub>4</sub>O<sub>15</sub> ceramics, *Ceram. Int.* 39 (6) (2013) 6991-6995.
- [18] M. Ohsahi, H. Ogawa, A. Kan, E. Tanaka, Microwave dielectric properties of low-temperature sintered Li<sub>3</sub>AlB<sub>2</sub>O<sub>6</sub> ceramic, *J. Eur. Ceram. Soc.* 25 (12) (2005) 2877-2881.
- [19] B.H. Jung, S.J. Hwang, H.S. Kim, Glass-ceramic for low temperature co-fired dielectric ceramic materials based on La<sub>2</sub>O<sub>3</sub>-B<sub>2</sub>O<sub>3</sub>-TiO<sub>2</sub> glass with BNT ceramics, *J. Eur. Ceram. Soc.* 25 (13) (2005) 3187-3193.
- [20] M. Udrovic, M. Valant, D. Suvorov, Dielectric characterization of ceramics from the TiO<sub>2</sub>-TeO<sub>2</sub> system, *J. Eur. Ceram. Soc.* 21 (10-11) (2001) 1735-1738.